

Article

Synthesis and Dynamic Behavior of Ce(IV) Double-Decker Complexes of Sterically Hindered Phthalocyanines

Jeevithra Dewi Subramaniam ¹, Toshio Nishino ^{1,*}, Kazuma Yasuhara ^{1,2} and Gwénaél Rapenne ^{1,3,*}

¹ Division of Materials Science, Nara Institute of Science and Technology, 8916-5 Takayama, Ikoma 630-0192, Japan

² Center for Digital Green-Innovation, Nara Institute of Science and Technology, 8916-5 Takayama, Ikoma 630-0192, Japan

³ Centre d'Elaboration de Matériaux et d'Etudes Structurale, Université de Toulouse, CNRS, 29, Rue Marvig, 31055 Toulouse, France

* Correspondence: t-nishino@ms.naist.jp (T.N.); gwenaël-rapenne@ms.naist.jp (G.R.)

Abstract: Phthalocyanines and their double-decker complexes are interesting in designing rotative molecular machines, which are crucial for the development of molecular motors and gears. This study explores the design and synthesis of three bulky phthalocyanine ligands functionalized at the α -positions with phenothiazine or carbazole fragments, aiming to investigate dynamic rotational motions in these sterically hindered molecular complexes. Homoleptic and heteroleptic double-decker complexes were synthesized through the complexation of these ligands with Ce(IV). Notably, Ce^{IV}(Pc₂)₂ and Ce^{IV}(Pc₃)₂, both homoleptic complexes, exhibited blocked rotational motions even at high temperatures. The heteroleptic Ce^{IV}(Pc)(Pc₃) complex, designed to lower symmetry, demonstrated switchable rotation along the pseudo-C₄ symmetry axis upon heating the solution. Variable-temperature ¹H-NMR studies revealed distinct dynamic behaviors in these complexes. This study provides insights into the rotational dynamics of sterically hindered double-decker complexes, paving the way for their use in the field of rotative molecular machines.

Keywords: double-decker complex; homoleptic; heteroleptic; cerium ion; ligand rotation; phthalocyanine; carbazole; phenothiazine



Citation: Subramaniam, J.D.; Nishino, T.; Yasuhara, K.; Rapenne, G.

Synthesis and Dynamic Behavior of Ce(IV) Double-Decker Complexes of Sterically Hindered Phthalocyanines. *Molecules* **2024**, *29*, 888. <https://doi.org/10.3390/molecules29040888>

Academic Editor: Andrea Bencini

Received: 22 January 2024

Revised: 8 February 2024

Accepted: 15 February 2024

Published: 17 February 2024



Copyright: © 2024 by the authors. Licensee MDPI, Basel, Switzerland. This article is an open access article distributed under the terms and conditions of the Creative Commons Attribution (CC BY) license (<https://creativecommons.org/licenses/by/4.0/>).

1. Introduction

Phthalocyanines (Pc) [1] represent a class of porphyrinoids that possess intriguing electronic, optical, and magnetic properties [2]. Thanks to their unique structural features and versatile properties, they are widely used as a building block in various functional materials, such as molecular electronics [3], dyes [4], photovoltaic devices [5], and advanced catalysts [6]. Phthalocyanines can coordinate to various metal ions in their central cavity of a macrocyclic structure composed of four isoindoles bridged by nitrogen atoms. Their coordination ability is not limited to alkaline metals, alkaline earth metals, and transition metals, but also to rare-earth ions. In particular, phthalocyanines form double-decker complexes with metal ions with large ionic radii like Cd, Hg, and rare-earth ions, in which the metal ion is sandwiched with two phthalocyanines [7,8]. These double-decker complexes exhibit unique molecular properties such as multistep redox properties [9–11], single molecular magnetism [11,12], and photocatalytic properties [13] which are derived from metal– π and π – π interactions. Moreover, the three-dimensional architecture of these double-decker structures makes them versatile building blocks for designing molecular machines with rotary units capable of controlled motion at the molecular level such as molecular motors and gears [14–19].

The first demonstration of rotation behavior in solution involving phthalocyanine macrocycles was reported in 2011 by Otsuki et al. [20]. They studied a two-fold symmetric heteroleptic double-decker complex with a meso-substituted porphyrin and a Pc ligand

coordinated to a Ce(IV) ion. The inter-ring rotation was observed as a flip by 90° from one antiprismatic geometry to another as evidenced by variable-temperature NMR. In 2023, Martynov et al. published the intramolecular rotation of Y(III) phthalocyaninates by analyzing the change in the conformational behavior, also using variable-temperature NMR [21]. However, the effect of the bulkiness of peripheral substituents on the rotative motion around the central metal ion of double-decker complexes was not well investigated for bis(phthalocyanato) double-decker complexes since the regio-controlled functionalization and desymmetrization of phthalocyanines are more difficult compared with porphyrins. This work specifically focuses on the formation of double-decker complexes using bulky Pc [20,22–26]. The aim is to investigate the dynamic rotation motions under thermal influence in these sterically hindered molecular complexes.

Here, we report the design and synthesis of three bulky Pc ligands functionalized at the α -positions with four *tert*-butyl phenothiazine (**H₂Pc1**) or four *tert*-butyl carbazole (**H₂Pc2**). Furthermore, a desymmetrized A₃B phthalocyanine (**H₂Pc3**) was also prepared with one phenothiazine and three *tert*-butyl carbazole substituents. These ligands were used to synthesize two homoleptic and one heteroleptic double-decker complexes through the complexation of these Pc with Ce^{IV}. The internal rotating motions of these complexes were studied in solution using variable-temperature ¹H-NMR (VT-¹H-NMR).

2. Results and Discussion

2.1. Molecular Design of Sterically Hindered Double-Decker Complexes

Double-decker complexes with sterically hindered peripheral substituents, wherein a lanthanoid ion is sandwiched between two Pc ligands (Figure 1) can serve as valuable structural motifs for the study of intramolecular rotating motions since the ligands can rotate around the metal center (axis of rotation shown in Figure 1). To examine the impact of bulkiness on the formation of double-decker complexes and the dynamics of their rotating motions, we designed Pc ligands functionalized at the α -positions with the planar bulky substituents 3,6-di-*tert*-butyl phenothiazine and 3,6-di-*tert*-butyl carbazole. The *tert*-butyl groups are present here to improve the solubility of the target ligands and double-decker complexes.

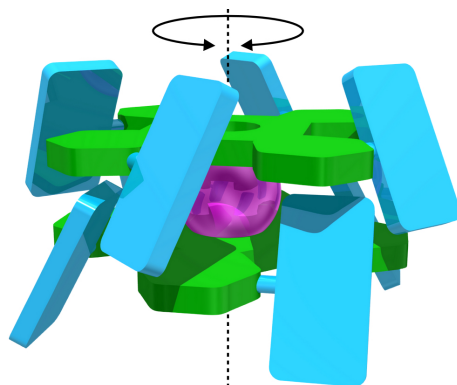


Figure 1. Schematic design of the sterically hindered double-decker complex of this work with the axis of rotation of interest (the main axis of rotation is given as a dashed line). The phthalocyanine rings are shown in green, the lanthanoid ion in purple, and the planar bulky substituents in blue.

2.2. Synthesis of the Pc Ligands Functionalized at the α -Positions with Bulky Groups

The cyclic tetramerization of mono-substituted phthalonitrile can produce a mixture of four distinct regioisomers with C_{4h}, C_s, C_{2v}, and D_{2h} symmetries, as illustrated in Figure 2. It has been firmly established that introducing bulky substituents at the 3-position of phthalonitrile selectively yields the C_{4h} isomer [22]. The reaction progresses through heating the phthalonitrile in a solution of lithium octanoate in n-octanol [27].

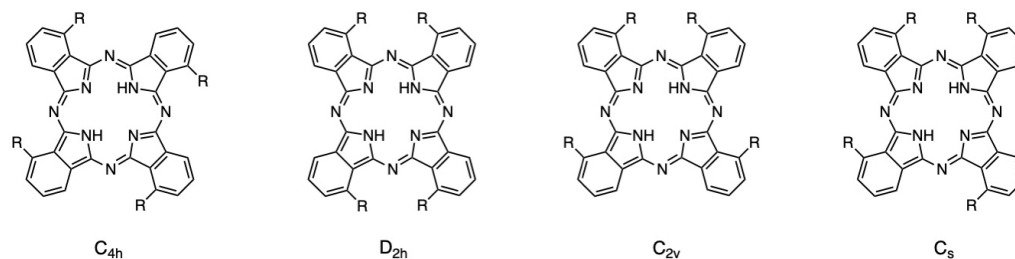


Figure 2. Regioisomers of the Pc ring obtained by cyclic tetramerization of 3-substituted phthalonitrile.

Two symmetric A4 phthalocyanine ligands with four 3,7-di-*tert*-butyl phenothiazines (**H₂Pc1**) or four 3,6-di-*tert*-butyl carbazoles (**H₂Pc2**) at the α -position were synthesized. Moreover, a desymmetrized A3B phthalocyanine (**H₂Pc3**) was also prepared with one phenothiazine and three 3,6-di-*tert*-butyl carbazole substituents (Figure 3).

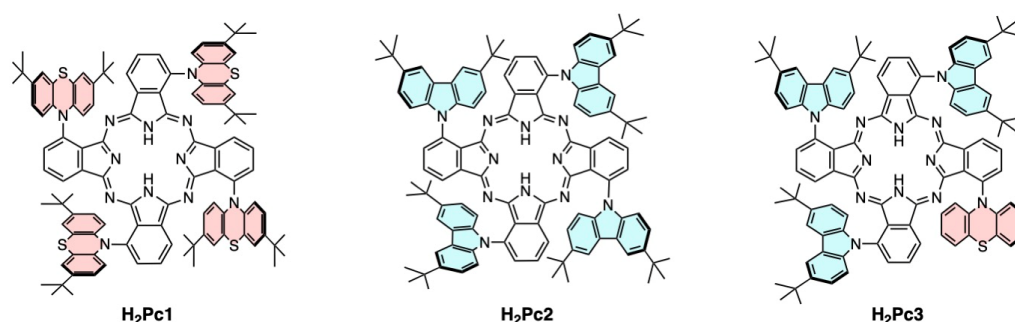


Figure 3. The three Pc ligands synthesized by tetramerization of phthalonitrile precursors.

2.2.1. Symmetric A4 Pc Ligands **H₂Pc1** and **H₂Pc2**

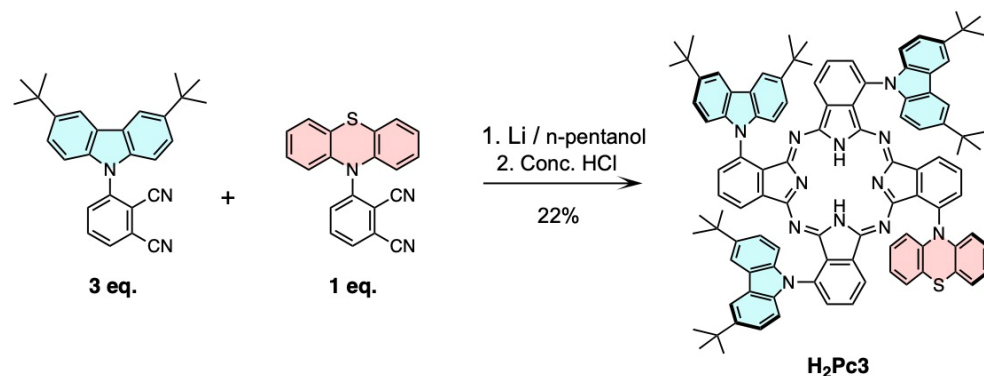
The synthesis of the phenothiazine-substituted phthalonitrile was achieved in two steps. Firstly, 3,6-di-*tert*-butyl phenothiazine was synthesized in 79% yield via a double Friedel–Crafts alkylation of phenothiazine with AlCl₃ [28] followed by the N-arylation of the phenothiazine by 3-fluorophthalonitrile in the presence of NaH [29]. The 3,6-di-*tert*-butyl carbazolyphthalonitrile was obtained by following a modified published procedure [19]. Tetramerization of the phthalonitriles selectively gave the C_{4h} symmetric Li₂Pc ligands through Li template synthesis. The metal-free **H₂Pc1** and **H₂Pc2** were then quantitatively obtained by demetallation of the lithium ions by reaction with concentrated HCl. The formation of the Pc ligands functionalized at the α -positions was confirmed by ¹H-NMR and MS (Figures S1–S3). In particular, the ¹H-NMR spectra revealed that, as expected, only one isomer was selectively obtained. Generally, Pc ligands tend to easily aggregate in solution, resulting in broad signals. Surprisingly, for these bulky ligands, the signals are sharp, indicating the difficulty for the aromatic rings to interact closely.

2.2.2. Disymmetric A3B Pc Ligand **H₂Pc3**

To facilitate the tracking of the rotation, we envisioned the preparation of a disymmetric A3B Pc ligand [30]. For this purpose, alongside three 3,6-di-*tert*-butyl carbazole subunits, we selected the phenothiazine fragment as the chemical tag to complete the molecular structure.

The desymmetrized **H₂Pc3** ligand was synthesized via a statistical condensation reaction. Six different compounds could be obtained, A4, A3B, A2B2 (cis and trans isomers), AB3, and B4, in a statistical distribution. Since the two dinitrile compounds are expected to exhibit comparable reactivity, employing a strict 3:1 molar ratio of each dinitrile favors the formation of the desired A3B compound with a statistical yield of 44% followed by the symmetric A4 compound (33%) and the remaining cis and trans A2B2, AB3, and B4 as minor products [31]. **H₂Pc3** was obtained by heating a mixture of 3,6-di-*tert*-butyl-carbazole phthalonitrile with 3-phenothiazine phthalonitrile in a 3:1 molar ratio in lithium pentoxide

in *n*-pentanol at reflux for 21 h (Scheme 1). Purification of the mixture by silica column chromatography yielded the desired compound in 22% yield.



Scheme 1. Synthesis of the disymmetric H_2Pc3 ligand based on a statistical condensation reaction.

2.3. Synthesis of the Double-Decker Cerium(IV) Complexes

Figure 4 presents the three double-deckers synthesized in this work. $Ce^{IV}(Pc2)_2$ and $Ce^{IV}(Pc3)_2$ are homoleptic while $Ce^{IV}(Pc)(Pc3)$ is heteroleptic.

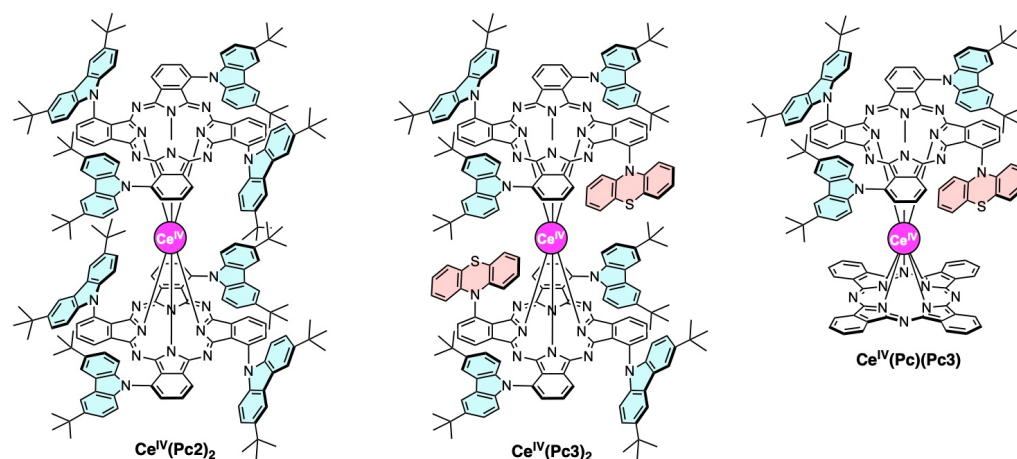


Figure 4. The three double-decker complexes synthesized by coordination with a cerium(IV) ion.

2.3.1. Homoleptic Double Deckers $Ce^{IV}(Pc2)_2$ and $Ce^{IV}(Pc3)_2$

Firstly, we attempted the synthesis of the homoleptic double-deckers with the three bulky Pc ligands shown Figure 3, using the microwave conditions described by H.G. Jin et al. [32].

The reaction of H_2Pc1 with $Ce(acac)_3 \cdot nH_2O$ was initially attempted using microwave heating in three cycles of 1 h at 270 °C, but only the starting material was quantitatively recovered, as confirmed by 1H -NMR data. A second attempt by refluxing H_2Pc1 with the same cerium source in *n*-octanol for 8 h also failed, possibly due to excessive steric hindrance between the phenothiazine groups of two different ligands. To validate this hypothesis, we attempted to form the double-decker complex with the less hindered H_2Pc2 . Connected through a nitrogen atom involved in a five-membered cycle (instead of a central six-membered ring for the phenothiazine fragment), the carbazole sub-unit is less sterically hindered. Under the same reaction conditions using microwave heating, the less hindered H_2Pc2 successfully coordinated to the Ce(IV). The reaction was quenched with MeOH, and the precipitate obtained was purified by silica column chromatography and recycling GPC, followed by recrystallization to yield the double-decker complex $Ce^{IV}(Pc2)_2$ in 70% yield.

In addition to giving neutral double-decker complexes, cerium (IV) is also one of the lanthanide ions that exhibit diamagnetism in double-decker structures [7]. Pc functionalized at the four α -positions is prochiral. Once coordinated in a double-decker architecture, as depicted in Figure 5, three stereoisomers can be envisioned [33]: one pair of enantiomers

(R-R and S-S) and a meso (R-S). It is expected that the (R-S) meso form would be obtained as the main product since the steric hindrance is reduced between the upper and lower substituents [34].

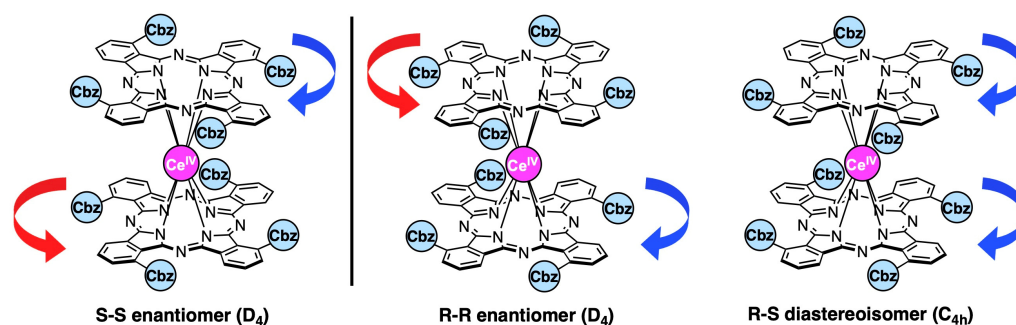


Figure 5. Possible stereoisomers of double-decker complex formed from a Pc functionalized at the four α -positions: R,R and S,S enantiomers as well as the R,S meso diastereomer (Cbz = 3,6-di-*tert*-butyl-carbazole).

Single crystals suitable for X-ray diffraction analysis were obtained by a slow diffusion of methanol into a chloroform solution of the complex. Their analysis confirms the formation of the expected (R-S) meso stereoisomer of the sterically crowded double-decker complex $\text{Ce}^{\text{IV}}(\text{Pc}2)_2$. The cerium center is coordinated by eight nitrogen atoms of the $\text{Pc}2$, forming a distorted square antiprismatic coordination geometry with a twisting angle of 33° (Figure 6).

The sterically hindered ligand drastically modifies this angle, which is usually about 45° in homoleptic double-decker complexes of Pc [19,33]. Similar to the structures of many double-decker complexes, the two ligands are not strictly planar and display a saucer shape. This structure reveals that peripheral carbazoles are arranged in a herringbone manner compared to each other. The carbazole substituents of both Pc rings are not perpendicular to the average plane of the Pc rings but are tilted at $+52^\circ$ in one Pc ring and -48° in the other one. This herringbone arrangement of carbazoles in the crystal could be due to the T-shaped π - π interaction between neighboring carbazoles.

From the $^1\text{H-NMR}$ spectrum of $\text{Ce}^{\text{IV}}(\text{Pc}2)_2$ depicted in Figure 7, it is clear that a major isomer is present, with less intense signals corresponding to minor stereoisomers (R-R and S-S). The MS data (Figure S11) revealed a single peak corresponding to $\text{Ce}^{\text{IV}}(\text{Pc}2)_2$ exhibiting the anticipated isotopic pattern and the absence of free ligands or triple-deckers.

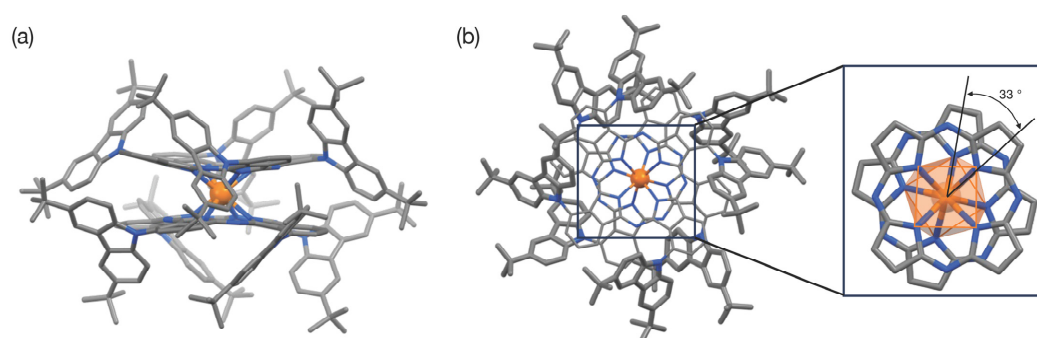


Figure 6. Side view (a) and top view (b) of the single crystal structure of $\text{Ce}^{\text{IV}}(\text{Pc}2)_2$. Hydrogens are omitted for clarity. Ce is in orange, N in blue and C in grey.

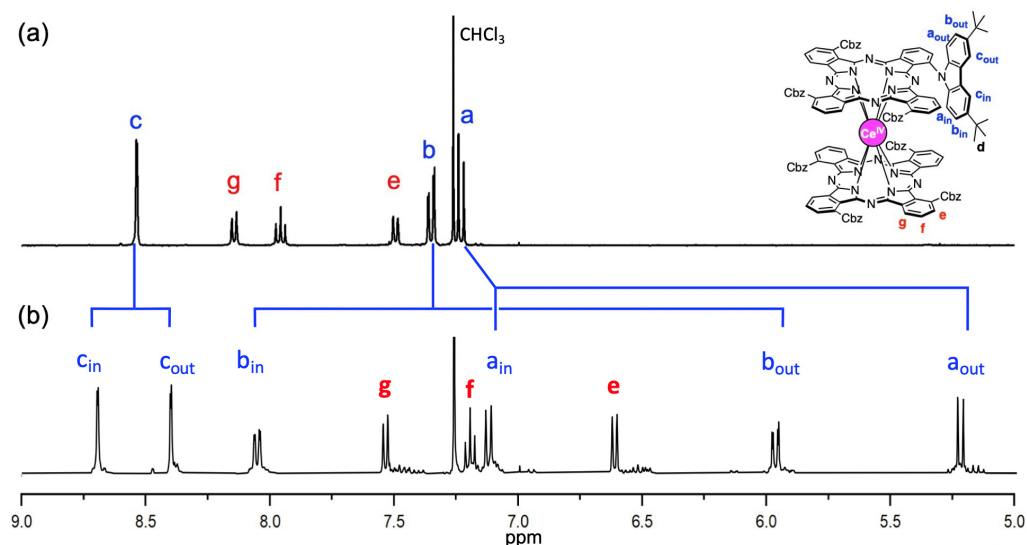


Figure 7. $^1\text{H-NMR}$ spectra of (a) H_2Pc_2 and (b) $\text{Ce}^{\text{IV}}(\text{Pc}_2)_2$ in CDCl_3 (400 MHz). The full assignments of the signals (indicated with letters in the molecule shown top right) were made with the assistance of COSY (Figure S9).

Following complexation, the carbazole protons are no longer equivalent due to restricted rotation along the C-N bond at room temperature. Consequently, the carbazole signals are split into two groups, as illustrated in Figure 7, with one part of the carbazole on the side of the Ce(IV) center while the second part is outside. It is known from the literature that the *in* signals are shifted downfield and the *out* signals are shifted upfield due to the strong ring current generated by the porphyrinoid ligands [35,36]. Consequently, the aromatic protons of the carbazole resonate can be divided into two groups, *in* and *out*, with signals for H_a at 7.12 ppm (*in*) and 5.23 ppm (*out*), for H_b at 8.05 ppm (*in*) and 5.97 ppm (*out*), and for H_c at 8.69 ppm (*in*) and 8.40 ppm (*out*). Additionally, the protons of the Pc ring resonate at 7.54 ppm (H_g), 7.21 ppm (H_f), and 6.62 ppm (H_e). A similar effect is observed for the *tert*-butyl protons with two singlets at 1.86 and 1.02 ppm (Figure S7).

Increasing the temperature did not change the spectrum, indicating that the carbazole substituents cannot freely rotate, which is not surprising considering the X-ray structure. As this complex is prepared from two symmetrical Pc_2 ligands, we cannot be certain if there is a rotation of the Pc ring around its C_4 symmetry axis, as the spectrum remains the same with or without rotation. To obtain such information, we investigated the rotation in a double-decker with comparable steric hindrance, prepared using two desymmetrized Pc_3 ligands.

$\text{Ce}^{\text{IV}}(\text{Pc}_3)_2$ complexation was carried out by following the same strategy. The formation of the complex was confirmed by MALDI-TOF-MS with the expected molecular ion peaks and isotopic distribution. The $^1\text{H-NMR}$ spectrum at room temperature was very complex due to the presence of many rotamers (Figure S12). Unfortunately, even at high temperature (140 °C), no changes have been observed (Figure S13). This indicates that the energy barrier is too large in this sterically overcrowded system, preventing any rotation around the pseudo- C_4 symmetry axis.

2.3.2. Heteroleptic Double-Decker $\text{Ce}^{\text{IV}}(\text{Pc})(\text{Pc}_3)$

Since $\text{Ce}^{\text{IV}}(\text{Pc}_3)_2$ was unsuitable for studying rotational motions due to the tight engagement of the upper and lower decks, we prepared a heteroleptic Ce^{IV} double-decker complex with Pc_3 and the unfunctionalized Pc. Lowering the symmetry of the phthalocyanine ring is crucial for fine-tuning the physicochemical properties [30] but also to facilitate the tracking of rotation. There are only a few examples in the literature of heteroleptic double-decker complexes incorporating one desymmetrized Pc ring [7,37–39].

To prepare the heteroleptic double-decker complex, one equivalent of $\text{H}_2\text{Pc3}$ and one equivalent of H_2Pc were reacted with $\text{Ce}(\text{acac})_3 \cdot n\text{H}_2\text{O}$ using microwave in *o*-DCB at 270 °C. This reaction led to a mixture of three compounds, with two homoleptic complexes, $\text{Ce}^{\text{IV}}(\text{Pc3})_2$ and $\text{Ce}^{\text{IV}}(\text{Pc})_2$, and the desired complex, $\text{Ce}^{\text{IV}}(\text{Pc})(\text{Pc3})$, obtained with a yield of 37% after column chromatography. Their structures were confirmed by $^1\text{H-NMR}$ and MS with the expected molecular ion peaks and isotopic distribution (Figure S18).

2.4. $^1\text{H-NMR}$ Studies of the Dynamic Internal Rotating Motions in $\text{Ce}^{\text{IV}}(\text{Pc})(\text{Pc3})$

The rotational flexibility of double-decker structures has been a subject of notable interest. Extensive studies employing variable-temperature $^1\text{H NMR}$ have been conducted on lanthanoid and zirconium (IV) double-decker complexes [20,21]. In 2000, Aida and co-workers investigated this type of intramolecular rotation using chiral cerium(IV) and zirconium(IV) double-decker complexes of an ABAB porphyrin ring [40]. The ligand rotation in these double-decker complexes was largely influenced by the steric hindrance of the substituent and the central metal atom. To the best of our knowledge, the dynamic behavior of heteroleptic double-decker complexes comprising an A3B Pc ring with highly sterically hindered perpendicular substituents has not been reported.

The $^1\text{H-NMR}$ spectrum of $\text{Ce}^{\text{IV}}(\text{Pc})(\text{Pc3})$ is very complex as revealed by the number of signals (Figure S15). As expected, the aromatic region of the spectrum contains a large number of well-resolved signals but also some overlapped and broad signals. Due to the low symmetry and the lack of rotation around the metal center, all the protons are inequivalent, even the four subunits of the unfunctionalized Pc.

The total integration of all aromatic signals fits well with the number of aromatic protons (54H) and the *tert*-Bu protons (also 54H). The *tert*-Bu signals are divided into two groups, with three singlets at around 1 ppm (*out*) and three singlets at around 2 ppm (*in*). Thus, variable-temperature NMR spectroscopy has been measured in the range of -20 to 120 °C (Figure S16) to see if the rotation processes around the axis shown in green and blue in Figure 8 can be investigated. Firstly, the *tert*-Bu signals are still divided into two groups (Figure 8c), even at high temperatures, which means the carbazole substituents cannot fully rotate around the C-N bond of the carbazole functionalization (green axis). They are just oscillating faster, inducing a shift for some singlets. A full and fast rotation would have given one set of three singlets without discrimination of the *in* and the *out* *tert*-butyl groups.

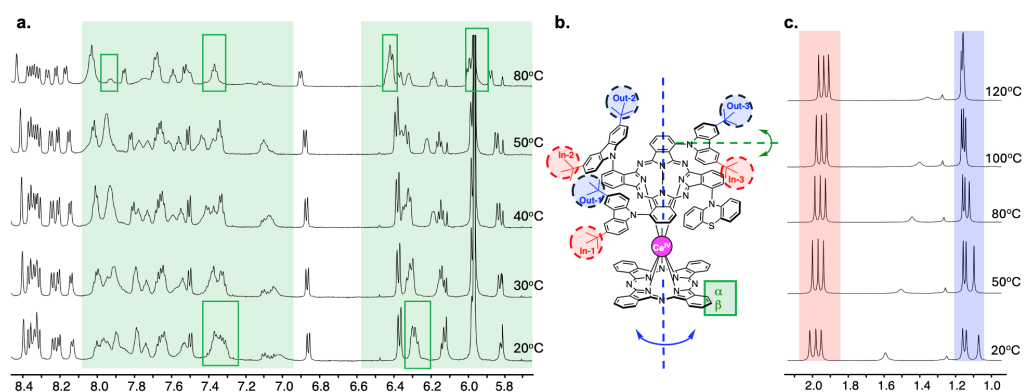


Figure 8. VT- $^1\text{H-NMR}$ spectra of $\text{Ce}^{\text{IV}}(\text{Pc})(\text{Pc3})$ in $\text{C}_2\text{D}_2\text{Cl}_4$ (600 MHz): (a) In the aromatic region, the signals corresponding to the α and β protons (green region) are shifted and simplified at higher temperatures. (b) The molecular structure with the color code of the discussed protons; in red and blue are the *in* and *out* *tert*-butyl protons, and in green is the Pc protons. (c) In the aliphatic region, the signals corresponding to the *tert*-butyl protons are splitted in two groups. While the *in* signals are not changed, The blue and green arrows correspond to the rotation axis around the pseudo- C_4 symmetry axis (blue-dotted axis) and the C-N bound axis between the phthalocyanine and carbazole (green-dotted axis).

The expected 18 signals for the carbazole sub-units and the 8 signals for the phenothiazine sub-unit were all identified (Figure S15). The remaining aromatic protons, therefore, arise from the α and β protons of the two Pc rings. Sixteen protons were sharp while twelve were shown to be broad, sometimes visible or overlapping with other signals. The signals correlating by group of three protons (from the ^1H - ^1H COSY experiment) correspond to the functionalized Pc ring, and the signals correlating by group of four protons were assigned to the unfunctionalized Pc. The broad signals could be due to a slow exchange between different conformers due to the rotation of the ligands around the cerium ion [21]. A full and fast rotation would have given only one signal for each of the α and β protons. In our case, even at high temperature we can notice that the signals corresponding to the α and β protons are shifted and simplified (Figure 8a, green region) but remain as more than two signals, which means the unfunctionalized Pc ring is rotating faster at high temperature, but is still slower than the NMR timescale.

3. Materials and Methods

3.1. General Informations

All reagents and solvents were purchased at the highest commercial quality available and used without further purification, unless otherwise stated. Anhydrous tetrahydrofuran, hydrochloric acid, and chloroform were purchased from FUJIFILM Wako Pure Chemical Corporation (Osaka, Japan). Lithium and $\text{Ce}(\text{acac})_3 \cdot n\text{H}_2\text{O}$ were purchased from Sigma Aldrich (St. Louis, MO, USA). Dichloromethane and phenothiazine were purchased from Nacalai tesque, Inc. (Kyoto, Japan). 3-fluorophthalonitrile and 3,6-di-*tert*-butyl-9H-carbazole were purchased from BLD Pharmatech Ltd. (Shanghai, China). Aluminium(III) chloride was purchased from TCI (Tokyo, Japan).

Silica gel column chromatography and thin-layer (TLC) chromatography were performed using Wakosil[®] 60 and Merck silica gel 60 (F254) TLC plates, respectively. ^1H and ^{13}C NMR spectra were recorded on a JEOL JNM-ECA600 (600 MHz for ^1H ; 150 MHz for ^{13}C) spectrometer, a JEOL JNM-ECZ500 (500 MHz for ^1H ; 125 MHz for ^{13}C) spectrometer, or a JEOL JNM-ECX400P (400 MHz for ^1H ; 100 MHz for ^{13}C) spectrometer at a constant temperature of 25 °C unless otherwise specified. Tetramethylsilane (TMS) was used as an internal reference for ^1H and ^{13}C -NMR measurements in CDCl_3 and $\text{C}_2\text{D}_2\text{Cl}_2$. A residual peak of a solvent was used as an internal reference for ^1H -NMR measurements in CD_2Cl_2 , *o*-DCB- d_4 , and $\text{DMSO}-d_6$, and chemical shifts (δ) are reported in ppm. Coupling constants (J) are given in Hz and the following abbreviations are used to describe the signals: singlet (s); broad singlet (br. s); doublet (d); triplet (t); quadruplet (q); quintuplet (qt); and multiplet (m). Full assignments of ^1H -NMR spectra were made with the assistance of COSY. The numbering system used for the assignment of signals is provided along with the corresponding spectra in the supporting information. The EI mass spectrometry was performed using JEOL AccuTOF JMS-T100LC. MALDI-TOF mass spectrometry was performed using a JEOL JMS-S3000 spectrometer. CEM Discover SP was used for reactions using a microwave irradiator. Single-crystal X-ray structure analysis was performed using Rigaku ValiMax RAPID (Rigaku, Tokyo, Japan).

3.2. Synthesis

3.2.1. Homoleptic Cerium(IV) Double-Decker Complex $\text{Ce}^{\text{IV}}(\text{Pc}2)_2$

In a 10 mL microwave vial, $\text{H}_2\text{Pc}2$ (0.81 g, 1.6 eq., 500 μmol) and $\text{Ce}(\text{acac})_3 \cdot n\text{H}_2\text{O}$ (0.17 g, 1 eq., 382 μmol) was mixed in 5 mL of *o*-DCB. N_2 was purged into the mixture and the sample was irradiated with microwave at 270 °C for 3 cycles of 1 h. The reaction was monitored after each cycle by TLC in hexane/ CH_2Cl_2 (7:3). After precipitation with MeOH and filtration, the collected solid was purified by column chromatography on silica eluted with CH_2Cl_2 . The three stereoisomers give only one spot on TLC ($R_f = 0.37$ in hexane/ CH_2Cl_2 3:1). A green compound was further purified by recycling GPC (JAIGEL 2H-2.5H; eluent: CHCl_3), followed by recrystallization with CHCl_3 and MeOH to obtain $\text{Ce}^{\text{IV}}(\text{Pc}2)_2$ in 70% yield (0.60 g). ^1H -NMR (400 MHz, CDCl_3): δ 8.69 (d, $J = 1.2$ Hz, 8H,

c_{in}), 8.40 (d, $J = 2.0$ Hz, 8H, c_{out}), 8.05 (dd, $J = 1.6, 8.4$ Hz, 8H, b_{in}), 7.53 (d, $J = 7.2$ Hz, 8H, g), 7.19 (t, 8H, f), 7.12 (d, $J = 8.4$ Hz, 8H, a_{in}), 6.61 (d, $J = 7.6$ Hz, 8H, e), 5.97 (dd, $J = 1.6, 8.8$ Hz, 8H, b_{out}), 5.23 (d, $J = 8.4$ Hz, 8H, a_{out}), 1.86 (s, 72H, d_{in}), 1.02 (s, 72H, d_{out}). ^{13}C NMR (100MHz, $CDCl_3$): 156.2, 154.2, 143.0, 142.1, 140.2, 139.6, 136.3, 132.6, 131.8, 129.9, 127.1, 124.1, 123.8, 122.3, 115.9, 115.1, 111.5, 111.2, 35.3, 34.4, 32.7, 31.8. UV-vis ($CHCl_3$) λ_{max} (ϵ): 298 (159,090), 334 (110,460), 566 (23,360), 635 (sh, 29,440), 700 (113,230). HR-MS (MALDI-TOF-MS): m/z calculated for $[Ce^{IV}(Pc_2)_2]^+$ ($C_{224}H_{216}N_{24}Ce$) 3381.6690; found 3381.6817. Elemental analysis: calcd. $C_{224}H_{216}N_{24}Ce$ (%): C(79.49), H(6.43), N(9.93); found (%): C(79.63), H(6.40), N(9.57).

3.2.2. Homoleptic Cerium(IV) Double-Decker Complex $Ce^{IV}(Pc_3)_2$

In a 10 mL microwave vial, H_2Pc_3 (0.10 g, 1.6 eq., 65 mmol) and $Ce(acac)_3 \cdot nH_2O$ (17 mg, 1 eq., 0.041 mmol) were mixed in 1 mL of *o*-DCB. After N_2 was purged into the mixture, the solution was irradiated with microwave at 270 °C for 3 cycles of 1 h. The reaction was monitored after each cycle by TLC in hexane/ CH_2Cl_2 (4:1). After precipitation with MeOH and filtration, the collected solid was purified by column chromatography on silica eluted with CH_2Cl_2 . The first eluted green band was collected and was subjected to size-exclusion column chromatography (Biobeads SX-1, $4\phi \times 65$ cm) with toluene. The dark blue compound in the first fraction corresponded to $Ce^{IV}(Pc_3)_2$ in 39% yield (51.5 mg) along with 28% (18 mg) of H_2Pc_3 in a second fraction (dark green). 1H -NMR: δ 8.89–5.27 (m), 4.68–4.32 (m), 2.11–1.74 (m, d_{in}), 1.28–0.95 (m, d_{out}). A complicated 1H -NMR spectrum was obtained due to many conformers. UV-vis ($CHCl_3$) λ_{max} (ϵ): 299 (91,380), 335 (76,310), 682 (65,190). HR-MS (MALDI-TOF-MS): m/z calculated for $[Ce^{IV}(Pc_3)_2]^+$ 3221.3627; found 3221.3639.

3.2.3. Heteroleptic Cerium(IV) Double-Decker Complex $Ce^{IV}(Pc)(Pc_3)$

In a 10 mL microwave vial, H_2Pc_3 (150 mg, 0.8 eq., 972 μ mol) and $Ce(acac)_3 \cdot nH_2O$ (53 mg, 1.0 eq., 121 μ mol) and $Ce(acac)_3 \cdot nH_2O$ (53 mg, 1.0 eq., 121 μ mol) were mixed in 2 mL of *o*-DCB. After N_2 was purged into the mixture, the solution was irradiated with microwave at 270 °C for 3 cycles of 1 h. The reaction was monitored after each cycle by TLC in hexane/ CH_2Cl_2 (1:1) and MALDI-TOF-MS. After precipitation with MeOH and filtration, the collected solid was purified by column chromatography on silica eluted with CH_2Cl_2 . The first eluted green band was collected and concentrated under reduced pressure. The compound with an R_f value of 0.26 was found to be the desired compound but a second column chromatography was necessary to purify it (SiO_2 , hexane/ CH_2Cl_2 1:1). Pure $Ce^{IV}(Pc)(Pc_3)$ was obtained with a yield of 37% (47.1 mg). 1H -NMR (600 MHz, $CDCl_3$): δ 8.82 (d, $J = 1.2$ Hz, 1H, c_{in}), 8.79 (d, $J = 1.2$ Hz, 1H, c_{in}), 8.66 (d, $J = 8.4$ Hz, 1H, a_{in}), 8.61 (d, $J = 8.4$ Hz, 1H, a_{in}), 8.63 (s, 1H, c_{in}), 8.48 (s, 1H, c_{out}), 8.44 (d, $J = 1.2$ Hz, 1H, c_{out}), 8.49 (s, 1H, αPc_3), 8.35 (d, $J = 1.2$ Hz, 1H, c_{out}), 8.34 (d, $J = 1.8$ Hz, 1H, b_{in}), 8.32 (s, 1H, a_{in}), 8.30 (dd, $J = 9.0$ Hz, 1.8 Hz, 1H, b_{in}), 8.23 (d, $J = 7.2$ Hz, 1H, βPc_3), 8.15–8.11 (m, 2H, b_{in} , αPc), 7.98 (d, $J = 7.2$ Hz, 1H, βPc_3), 7.89 (t, $J = 6.6$ Hz, 1H, βPc_3), 7.62–7.58 (m, 2H, βPc), 7.51 (t, $J = 7.2$ Hz, 1H, βPc_3), 7.43–7.33 (m, 2H, a_{out}), 7.36 (b, 1H, αPc), 7.28–7.22 (m, 1H, βPc), 7.24–7.28 (m, 1H, b_{out}), 6.82 (d, $J = 8.4$ Hz, 1H, k_{out}), 6.39 (d, $J = 9.0$ Hz, 1H, h_{in}), 6.35 (d, $J = 8.4$ Hz, 1H, k_{in}), 6.28 (d, $J = 8.4$ Hz, 1H, b_{out}), 6.24 (d, $J = 7.2$ Hz, 1H, αPc), 6.19 (d, $J = 6.6$ Hz, 1H, αPc_3), 6.10 (t, $J = 7.8$ Hz, 1H, j_{out}), 5.94 (d, $J = 7.2$ Hz, 1H, a_{out}), 5.94–5.88 (m, 2H, $i_{j_{out}}$), 5.44 (t, $J = 7.8$ Hz, 1H, i_{in}), 5.71 (d, $J = 8.4$ Hz, 1H, b_{in}), 4.63 (d, $J = 9.0$ Hz, 1H, h_{out}), 2.03 (s, 9H, $^tBu_{in}$), 2.00 (s, 9H, $^tBu_{in}$), 1.98 (s, 9H, $^tBu_{in}$), 1.21 (s, 9H, $^tBu_{out}$), 1.17 (s, 9H, $^tBu_{out}$), 1.15 (s, 9H, $^tBu_{out}$). ^{13}C NMR (150 MHz, CD_2Cl_2): 154.2, 154.1, 153.9, 153.6, 151.4, 151.2, 151.0, 150.7, 144.3, 143.4, 143.3, 143.1, 142.9, 142.1, 141.9, 141.1, 141.0, 141.0, 140.8, 138.8, 138.3, 138.0, 134.5, 133.1, 132.8, 132.5, 131.2, 131.1, 131.0, 130.9, 130.7, 130.5, 130.2, 127.4, 126.7, 126.0, 125.7, 124.7, 124.6, 124.3, 124.2, 124.1, 124.0, 123.7, 123.3, 121.8, 121.3, 120.8, 120.2, 119.7, 119.2, 118.7, 118.1, 117.6, 117.1, 116.6, 116.1, 115.5, 115.0, 114.5, 114.0, 113.4, 112.9, 112.4, 111.9, 111.3. UV-vis ($CHCl_3$) λ_{max} (ϵ): 298 (63,780), 571 (26,850),

668 (27,330), 740 (13,350). HR-MS (MALDI-TOF-MS): m/z calculated for $[\text{Ce}^{\text{IV}}(\text{Pc})(\text{Pc3})]^+$ 2192.7836; found 2192.7835.

4. Conclusions

In summary, three highly sterically hindered double-decker complexes have been prepared with phthalocyanines functionalized at the α -position despite their high steric hindrance. $\text{Ce}^{\text{IV}}(\text{Pc2})_2$ is a homoleptic complex of a tetrasubstituted Pc with carbazole and $\text{Ce}^{\text{IV}}(\text{Pc3})_2$ is a homoleptic complex of a desymmetrized Pc with three carbazoles and one phenothiazine. Since the rotative motions were blocked even at high temperatures in these homoleptic complexes, a heteroleptic $\text{Ce}^{\text{IV}}(\text{Pc})(\text{Pc3})$ complex was also prepared with one unfunctionalized ligand.

The dynamic behaviors of the $\text{Ce}^{\text{IV}}(\text{Pc3})_2$ and $\text{Ce}^{\text{IV}}(\text{Pc})(\text{Pc3})$ complexes were analyzed by VT-NMR from $-20\text{ }^\circ\text{C}$ to $140\text{ }^\circ\text{C}$. In the case of $\text{Ce}^{\text{IV}}(\text{Pc3})_2$, no change in the spectrum was observed, illustrating the too-high steric hindrance preventing any rotation from occurring. In the case of $\text{Ce}^{\text{IV}}(\text{Pc})(\text{Pc3})$, we demonstrated that rotation along the pseudo- C_4 symmetry axis can be switched on by heating the solution. The observed rotation is slow at room temperature, but as the temperature increases, some signals corresponding to the α - and β - protons of the Pc ligands appear as well-resolved signals. Additionally, the carbazole substituents do not fully rotate even at higher temperatures, but their faster oscillation allows the unfunctionalized Pc fragment to rotate, which was not possible in the case of the homoleptic complexes. We are now working on modifying such complexes to deposit them on a metallic surface to build a train of gears and observe the intermolecular transfer of rotating motions.

Supplementary Materials: The following supporting information can be downloaded at <https://www.mdpi.com/article/10.3390/molecules29040888/s1>: Figure S1: ^1H -NMR spectrum of $\text{H}_2\text{Pc1}$; Figure S2: ^{13}C NMR spectrum of $\text{H}_2\text{Pc1}$; Figure S3: HR-MALDI-TOF MS for $\text{H}_2\text{Pc1}$; Figure S4: ^1H -NMR of $\text{H}_2\text{Pc3}$; Figure S5: ^{13}C -NMR spectrum of $\text{H}_2\text{Pc3}$; Figure S6: HR-MALDI-TOF MS for $\text{H}_2\text{Pc3}$; Figure S7: ^1H -NMR spectrum of $\text{Ce}^{\text{IV}}(\text{Pc2})_2$; Figure S8: ^1H -NMR spectra of $\text{Ce}^{\text{IV}}(\text{Pc2})_2$ in $\text{C}_2\text{D}_2\text{Cl}_4$ at $20\text{ }^\circ\text{C}$ and $100\text{ }^\circ\text{C}$; Figure S9: COSY spectrum of $\text{Ce}^{\text{IV}}(\text{Pc2})_2$; Figure S10: ^{13}C -NMR spectrum of $\text{Ce}^{\text{IV}}(\text{Pc2})_2$ (CDCl_3 , 100MHz); Figure S11: HR-MALDI-TOF MS for $\text{Ce}^{\text{IV}}(\text{Pc2})_2$; Figure S12: ^1H -NMR spectrum of $\text{Ce}^{\text{IV}}(\text{Pc3})_2$; Figure S13: ^1H -NMR spectra of $\text{Ce}^{\text{IV}}(\text{Pc3})_2$ at $25\text{ }^\circ\text{C}$ and $140\text{ }^\circ\text{C}$; Figure S14: HR-MALDI-TOF MS for $\text{Ce}^{\text{IV}}(\text{Pc3})_2$; Figure S15: ^1H -NMR spectrum in $\text{C}_2\text{D}_2\text{Cl}_4$ (600 MHz) of $\text{Ce}^{\text{IV}}(\text{Pc})(\text{Pc3})$; Figure S16: Full VT- ^1H -NMR spectra of $\text{Ce}^{\text{IV}}(\text{Pc})(\text{Pc3})$ from -20 to $120\text{ }^\circ\text{C}$; Figure S17: ^{13}C -NMR spectrum of $\text{Ce}^{\text{IV}}(\text{Pc})(\text{Pc3})$; Figure S18: HR-MALDI-TOF MS for $\text{Ce}^{\text{IV}}(\text{Pc})(\text{Pc3})$; Figure S19: Picture of the crystal of $\text{Ce}^{\text{IV}}(\text{Pc2})_2$; Figure S20: ORTEP representation, table of crystal data and structure refinement for complex of $\text{Ce}^{\text{IV}}(\text{Pc2})_2$. Additional experimental section with the synthesis of $\text{H}_2\text{Pc1}$, $\text{H}_2\text{Pc2}$, and $\text{H}_2\text{Pc3}$; crystallographic data can be obtained free of charge from the Cambridge Crystallographic Data Centre via <https://www.ccdc.cam.ac.uk/structures/> (accessed on 14 February 2024). CCDC deposit numbers for double-decker complex $\text{Ce}^{\text{IV}}(\text{Pc2})_2$: 2324826.

Author Contributions: Conceptualization, J.D.S., T.N. and G.R.; synthesis and measurements, J.D.S., T.N. and G.R.; writing—original draft preparation, K.Y. and G.R.; writing—review and editing, T.N. and G.R.; funding acquisition, T.N. and G.R. All authors have read and agreed to the published version of the manuscript.

Funding: This research was funded by a JSPS KAKENHI Grant-in-Aid for Scientific Research (A) (number 22H00325, GR), a JSPS KAKENHI Grant-in-Aid for Challenging Research (number 20K21131, GR), and a JSPS KAKENHI Grant-in-Aid for Grant-in-Aid for Early-Career Scientists (number 23K13560, TN).

Institutional Review Board Statement: Not applicable.

Informed Consent Statement: Not applicable.

Data Availability Statement: The data presented in this study are available on request from the corresponding author.

Acknowledgments: Yoshiko Nishikawa is acknowledged for her contribution to the measurements of HR-MS spectra.

Conflicts of Interest: The authors declare no conflicts of interest.

References

1. Claessens, C.G.; Hahn, U.; Torres, T. Phthalocyanines: From outstanding electronic properties to emerging applications. *Chem. Rec.* **2008**, *8*, 75–97. [[CrossRef](#)]
2. Schmidt, A.M.; Calvete, M.J.F. Phthalocyanines: An old dog can still have new (photo)tricks! *Molecules* **2021**, *26*, 2823. [[CrossRef](#)]
3. Kong, X.; Zhang, X.; Gao, D.; Qi, D.; Chen, Y.; Jiang, J. Air-stable ambipolar field-effect transistor based on a solution-processed octanaphthoxy- substituted tris(phthalocyaninato) europium semiconductor with high and balanced carrier mobilities. *Chem. Sci.* **2015**, *6*, 1967–1972. [[CrossRef](#)]
4. Pekbelgin Karaoglu, H.; Kalkan Burat, A. α - and β -substituted metal-free phthalocyanines: Synthesis, photophysical and electrochemical properties. *Molecules* **2020**, *25*, 363. [[CrossRef](#)] [[PubMed](#)]
5. Bottari, G.; de la Torre, G.; Guldi, D.M.; Torres, T. Covalent and noncovalent phthalocyanine-carbon nanostructure systems: Synthesis, photoinduced electron transfer, and application to molecular photovoltaics. *Chem. Rev.* **2010**, *110*, 6768–6816. [[CrossRef](#)] [[PubMed](#)]
6. Sorokin, A.B. Phthalocyanine Metal Complexes in Catalysis. *Chem. Rev.* **2013**, *113*, 8152–8191. [[CrossRef](#)] [[PubMed](#)]
7. Martynov, A.G.; Horii, Y.; Katoh, K.; Bian, Y.; Jiang, J.; Yamashita, M.; Gorbunova, Y.G. Rare-earth based tetrapyrrolic sandwiches: Chemistry, materials and applications. *Chem. Soc. Rev.* **2022**, *51*, 9262–9339. [[CrossRef](#)] [[PubMed](#)]
8. Jiang, J.; Ng, D.K.P. A decade journey in the chemistry of sandwich-type tetrapyrrolo—Rare earth complexes. *Acc. Chem. Res.* **2009**, *42*, 79–88. [[CrossRef](#)] [[PubMed](#)]
9. Chabach, D.; Tahiri, M.; Cian, A.D.; Fischer, J.; Weiss, R.; El Malouli Bibout, E. Tervalent-Metal Porphyrin-Phthalocyanine Heteroleptic Sandwich-Type Complexes. Synthesis, Structure, and Spectroscopic Characterization of Their Neutral, Singly-Oxidized, and Singly-Reduced States. *J. Am. Chem. Soc.* **1995**, *117*, 8548–8556. [[CrossRef](#)]
10. Jiang, J.; Bian, Y.; Furuya, F.; Liu, W.; Choi, M.T.M.; Kobayashi, N.; Li, H.-W.; Yang, Q.; Mak, T.C.W.; Ng, D.K.P. Synthesis, Structure, Spectroscopic Properties, and Electrochemistry of Rare Earth Sandwich Compounds with Mixed 2,3-Naphthalocyaninato and Octaethylporphyrinato Ligands. *Chem. Eur. J.* **2001**, *7*, 5059–5069. [[CrossRef](#)] [[PubMed](#)]
11. Bian, Y.; Jiang, J.; Tao, Y.; Choi, M.T.M.; Li, R.; Ng, A.C.H.; Zhu, P.; Pan, N.; Sun, X.; Arnold, D.P.; et al. Tuning the Valence of the Cerium Center in (Na)phthalocyaninato and Porphyrinato Cerium Double-Deckers by Changing the Nature of the Tetrapyrrole Ligands. *J. Am. Chem. Soc.* **2003**, *125*, 12257–12267. [[CrossRef](#)]
12. Stepanow, S.; Honolka, J.; Gambardella, P.; Vitali, L.; Abdurakhmanova, N.; Tseng, T.; Rauschenbach, S.; Tait, S.L.; Sessi, V.; Klyatskaya, S.; et al. Spin and orbital magnetic moment anisotropies of monodispersed bis(phthalocyaninato)terbium on a copper surface. *J. Am. Chem. Soc.* **2010**, *132*, 11900–11901. [[CrossRef](#)] [[PubMed](#)]
13. Mele, G.; Garcia-López, E.; Palmisano, L.; Dyrda, G.; Słota, R. Photocatalytic Degradation of 4-Nitrophenol in Aqueous Suspension by Using Polycrystalline TiO₂ Impregnated with Lanthanide Double-Decker Phthalocyanine Complexes. *J. Phys. Chem. C* **2007**, *111*, 6581–6588. [[CrossRef](#)]
14. Gisbert, Y.; Abid, S.; Kammerer, C.; Rapenne, G. Molecular gears from solution to surfaces. *Chem. Eur. J.* **2021**, *27*, 12019–12031. [[CrossRef](#)]
15. Zhang, Y.; Kersell, H.; Stefak, R.; Echeverria, J.; Iancu, V.; Perera, G.; Li, Y.; Braun, K.F.; Joachim, C.; Rapenne, G.; et al. Simultaneous and coordinated rotational switching of all molecular rotors in a network. *Nat. Nanotech.* **2016**, *11*, 706–712. [[CrossRef](#)]
16. Michl, J.; Sykes, E.C.H. Molecular Rotors and Motors: Recent Advances and Future Challenges. *ACS Nano* **2009**, *3*, 1042–1048. [[CrossRef](#)]
17. Ikeda, M.; Takeuchi, M.; Shinkai, S.; Tani, F.; Naruta, Y. Synthesis of new diaryl-substituted triple-decker and tetraaryl-substituted double-decker lanthanum(III) porphyrins and their porphyrin ring rotational speed as compared with that of double-decker cerium(IV) porphyrins. *Bull. Chem. Soc. Jpn.* **2001**, *74*, 739–746. [[CrossRef](#)]
18. Miyake, K.; Fukuta, M.; Asakawa, M.; Hori, Y.; Ikeda, T.; Shimizu, T. Molecular motion of surface-immobilized double-decker phthalocyanine complexes. *J. Am. Chem. Soc.* **2009**, *131*, 17808–17813. [[CrossRef](#)]
19. Eciija, D.; Auwärter, W.; Vijayaraghavan, S.; Seufert, K.; Bischoff, F.; Tashiro, K.; Barth, J.V. Assembly and manipulation of rotatable cerium porphyrinato sandwich complexes on a surface. *Angew. Chem. Int. Ed.* **2011**, *50*, 3872–3877. [[CrossRef](#)]
20. Otsuki, J.; Taka, M.; Kobayashi, D. Rotational libration of a porphyrin/phthalocyanine double-decker complex with Ce(IV) as revealed by ¹H NMR and STM. *Chem. Lett.* **2011**, *40*, 717–719. [[CrossRef](#)]
21. Martynov, A.G.; Kirakosyan, G.A. Characterizing the conformational behavior of yttrium(III) tris-phthalocyaninates using VT-NMR spectroscopy. *Macromolecules* **2023**, *16*, 150–155. [[CrossRef](#)]
22. Yamamoto, S.; Kuribayashi, K.; Murakami, T.N.; Kwon, E.; Stillman, M.J.; Kobayashi, N.; Segawa, H.; Kimura, M. Regioregular phthalocyanines substituted with bulky donors at non-peripheral positions. *Chem. Eur. J.* **2017**, *23*, 15446–15454. [[CrossRef](#)]

23. Wang, R.; Li, Y.; Li, R.; Cheng, D.Y.Y.; Zhu, P.; Ng, D.K.P.; Bao, M.; Cui, X.; Kobayashi, N.; Jiang, J. Heteroleptic rare earth double-decker complexes with naphthalocyaninato and phthalocyaninato ligands. General synthesis, spectroscopic, and electrochemical characteristics. *Inorg. Chem.* **2005**, *44*, 2114–2120. [[CrossRef](#)] [[PubMed](#)]
24. Wang, R.; Li, R.; Li, Y.; Zhang, X.; Zhu, P.; Lo, P.C.; Ng, D.K.P.; Pan, N.; Ma, C.; Kobayashi, N.; et al. Controlling the nature of mixed (phthalocyaninato)(porphyrinato) rare-earth(III) double-decker complexes: The Effects of nonperipheral alkoxy substitution of the phthalocyanine ligand. *Chem. Eur. J.* **2006**, *12*, 1475–1485. [[CrossRef](#)] [[PubMed](#)]
25. Also for heteroleptic complexes Martynov, A.G.; Polovkova, M.A.; Bereznoy, G.S.; Sinelshchikova, A.A.; Khrustalev, V.N.; Birin, K.P.; Kirakosyan, G.A.; Gorbunova, Y.G.; Tsvadze, A.Y. Heteroleptic Crown-Substituted Tris(phthalocyaninates) as Dynamic Supramolecular Scaffolds with Switchable Rotational States and Tunable Magnetic Properties. *Inorg. Chem.* **2021**, *60*, 9110–9121. [[CrossRef](#)] [[PubMed](#)]
26. Birin, K.P.; Gorbunova, Y.G.; Tsvadze, A.Y. NMR investigation of intramolecular dynamics of heteroleptic triple-decker (porphyrinato)(phthalocyaninato) lanthanides. *Dalton Trans.* **2011**, *40*, 11474–11479. [[CrossRef](#)] [[PubMed](#)]
27. Li, R.; Zhang, X.; Zhu, P.; Ng, D.K.P.; Kobayashi, N.; Jiang, J. Electron-donating or -withdrawing nature of substituents revealed by the electrochemistry of metal-free phthalocyanines. *Inorg. Chem.* **2006**, *45*, 2327–2334. [[CrossRef](#)]
28. Sych, G.; Pashazadeh, R.; Danyliv, Y.; Bezhikonyi, O.; Volyniuk, D.; Lazauskas, A.; Grazulevicius, J.V. Reversibly switchable phase-dependent emission of quinoline and phenothiazine derivatives towards applications in optical sensing and information multicoding. *Chem. Eur. J.* **2021**, *27*, 2826–2836. [[CrossRef](#)]
29. Schoch, T.D.; Mondal, M.; Weaver, J.D. Catalyst-free hydrodefluorination of perfluoroarenes with NaBH₄. *Org. Lett.* **2021**, *23*, 1588–1593. [[CrossRef](#)]
30. Pushkarev, V.E.; Tolbin, A.Y.; Borisova, N.E.; Trashin, S.A.; Tomilova, L.G. A3B-type phthalocyanine-based homoleptic lanthanide(III) double-decker π -radical complexes bearing functional hydroxy groups: Synthetic approach, spectral properties and electrochemical study. *Eur. J. Inorg. Chem.* **2010**, 5254–5262. [[CrossRef](#)]
31. Göktuğ, Ö.; Soganci, T.; Ak, M.; Şener, M.K. Efficient synthesis of EDOT modified ABBB-type unsymmetrical zinc phthalocyanine: Optoelectronic and glucose sensing properties of its copolymerized film. *New J. Chem.* **2017**, *41*, 14080–14087. [[CrossRef](#)]
32. Jin, H.-G.; Jiang, X.; Kühne, I.A.; Clair, S.; Monnier, V.; Chendo, C.; Novitchi, G.; Powell, A.K.; Kadish, K.M.; Balaban, T.S. Microwave-mediated synthesis of bulky lanthanide porphyrin–phthalocyanine triple-deckers: Electrochemical and magnetic properties. *Inorg. Chem.* **2017**, *56*, 4864–4873. [[CrossRef](#)] [[PubMed](#)]
33. Yamada, Y.; Nakajima, H.; Kobayashi, C.; Shuku, Y.; Awaga, K.; Akine, S.; Tanaka, K. Synthesis of isomeric Tb³⁺-phthalocyanine double-decker complexes depending on the difference in the direction of coordination plane and their magnetic properties. *Chem. Eur. J.* **2023**, *29*, e202203272. [[CrossRef](#)]
34. Zhang, X.; Cai, X.; Qi, D.; Yao, P.; Bian, Y.; Jiang, J. Methoxy substituted heteroleptic bis(phthalocyaninato) yttrium complexes: Density functional calculations. *ChemPhysChem* **2008**, *9*, 781–792. [[CrossRef](#)] [[PubMed](#)]
35. Davoras, E.M.; Spyroulias, G.A.; Mikros, E.; Coutsolelos, A.G. Intramolecular dynamics of asymmetric lanthanide(III) porphyrin sandwich complexes in solution. ¹H-NMR spectroscopic elucidation of stereochemical effects of substituted cerium porphyrin double-deckers. *Inorg. Chem.* **1994**, *33*, 3430–3434. [[CrossRef](#)]
36. Babailov, S.P.; Coutsolelos, A.G.; Dikiy, A.; Spyroulias, G.A. Intramolecular Dynamics of Asymmetric Lanthanide(III) Porphyrin Sandwich Complexes in Solution. *Eur. J. Inorg. Chem.* **2001**, *2001*, 303–306. [[CrossRef](#)]
37. Pernin, D.; Habertho, K.; Simon, J. Novel unsymmetrical monofunctionalized lutetium and dysprosium bisphthalocyanines with seven crown-ether units and one hexyl hexanoate side-group. *J. Chem. Soc. Perkin 1* **1997**, 1265–1266. [[CrossRef](#)]
38. Sheng, N.; Li, R.; Choi, C.-F.; Su, W.; Ng, D.K.P.; Cui, X.; Yoshida, K.; Kobayashi, N.; Jiang, J. Heteroleptic bis(phthalocyaninato) europium(III) complexes fused with different numbers of 15-crown-5 moieties. Synthesis, spectroscopy, electrochemistry, and supramolecular structure. *Inorg. Chem.* **2006**, *45*, 3794–3802. [[CrossRef](#)]
39. Ballesteros, B.; de la Torre, G.; Shearer, A.; Hausmann, A.; Herranz, M.Á.; Guldi, D.M.; Torres, T. Lanthanide(III) bis(phthalocyaninato)-[60]fullerene dyads: Synthesis, characterization, and photophysical properties. *Chem. Eur. J.* **2010**, *16*, 114–125. [[CrossRef](#)]
40. Tashiro, K.; Konishi, K.; Aida, T. Metal bisporphyrinate double-decker complexes as redox-responsive rotating modules. Studies on ligand rotation activities of the reduced and oxidized forms using chirality as a Probe. *J. Am. Chem. Soc.* **2000**, *122*, 7921–7926. [[CrossRef](#)]

Disclaimer/Publisher’s Note: The statements, opinions and data contained in all publications are solely those of the individual author(s) and contributor(s) and not of MDPI and/or the editor(s). MDPI and/or the editor(s) disclaim responsibility for any injury to people or property resulting from any ideas, methods, instructions or products referred to in the content.